

Return-Point Memory in an Amorphous Solid

Nathan C. Keim,^{1,2,*} Jacob Hass,¹ Brian Kroger,¹ and Devin Wiekert¹

¹*Department of Physics, California Polytechnic State University, San Luis Obispo CA 93407, USA*

²*Kavli Institute for Theoretical Physics, Santa Barbara, CA 93106, USA*

(Dated: May 26, 2022)

A disordered material that cannot relax to equilibrium, such as an amorphous or glassy solid, responds to deformation in a way that depends on its past. In experiments we subject a 2D athermal amorphous solid to oscillatory shear that alternates between two amplitudes. We show that the system forms memories of both amplitudes, but only when the smaller one is applied last. This behavior, and the pattern of particle rearrangements as strain amplitude is varied, are consistent with the return-point memory seen in ferromagnets and many other systems. A simple model of a ferromagnet can reproduce the results of our experiments and of previous simulations. Unlike ferromagnets, amorphous solids' disorder is unquenched; they require “training” to develop this behavior.

We are familiar with our own memory and forgetfulness, and digital memories are woven into our lives. But all around us matter is being driven without relaxing to equilibrium, potentially forming memories of its own: specific information about past conditions that can be recalled later. As a simple example, rubber “remembers” the extrema of all deformations since it was cured [1]; the material stiffens as it is driven beyond those limits, allowing the memory to be read. Further afield, non-Brownian suspensions that are sheared cyclically [2, 3] and charge density-wave conductors given electrical pulses [4, 5] share distinctive rules for remembering multiple input values. Studying memory can thus reveal unexpected connections between systems and prompt new examinations of their physics.

Recently, a new memory behavior was discovered in amorphous solids [6]. This vast class of materials features atoms or particles packed with a minimum of the regular placement found in crystals. Amorphous solids made of molecules, bubbles, or macroscopic grains deform in remarkably similar ways: applied stress tends to cause localized clusters of particles to rearrange, marking transitions among a vast set of metastable states [7, 8]. Yet under oscillatory shear, after many cycles these materials' dynamics can become periodic; particles' trajectories become loops [6, 9–13]. Molecular dynamics simulations of glasses [6, 14, 15] and experiments on bubble rafts [16] showed that in this state, an amorphous solid retains an imprint of the amplitude of shearing that can be revealed with a suitable readout protocol. Moreover, when the strain amplitude of oscillatory shear was repeatedly switched between two values, both values could be recovered later.

These findings represent new possibilities for describing and exploiting these materials' complex history-dependence, but they also prompt new questions: What is the mechanism for memory formation and readout? What can memory reveal about the physics of amorphous solids more broadly? How should one place this behavior among examples of memory in other systems?

In this paper, we describe experiments with the two-dimensional amorphous solid in Fig. 1b. We demonstrate that when two amplitudes are applied there is a memory of each, but only when the smaller value was applied last before readout—a trait previously seen in systems with return-point memory (RPM). We then show that a simple model with RPM [17] can qualitatively explain previously published observations of memory in amorphous solids [6, 14, 15]. Furthermore, the detailed kinematics of this model as memories are encoded and read correspond to the rearrangements of particles in our experiments. By considering how RPM could arise in the physics of amorphous solids, we identify broader implications for studies of these materials and of memory.

Our experiment consists of polystyrene sulfate latex particles, with diameters 3.9 and 5.4 μm (Invitrogen), adsorbed at a decane-water interface (Fig. 1b) [12]. These particles exhibit long-range electrostatic repulsion [18], and so at the concentrations used here (area fraction ~ 0.25) each particle is mechanically over-constrained by its neighbors but does not touch them—forming a soft, frictionless jammed 2D solid [12, 19]. We use an interfacial shear rheometer [12, 20–22] to shear the material while imaging $\sim 40,000$ particles in a 1.4×1.9 mm area and tracking particles continuously [23, 24].

All of the experiments reported here follow the protocol: (1) a “reset” phase where we apply 6 cycles with strain amplitude $\gamma_0 \simeq 0.7$ at 0.1 Hz; (2) a “training” phase where we apply oscillatory shear at 0.05 Hz with a repeating pattern of strain amplitudes for 176 cycles, recording video for the last 24; (3) a “readout” phase. Figure 1a shows strain *vs.* time at the end of one experiment. In each cycle, strain follows sinusoidally the sequence $0 \rightarrow +\gamma_0 \rightarrow 0 \rightarrow -\gamma_0 \rightarrow 0$. Training involves the pattern of amplitudes $\gamma_1, \gamma_1, \gamma_1, \gamma_1, \gamma_2, \gamma_2, \gamma_2, \gamma_2$ (176 cycles = 22 pattern repetitions). The choice of $\gamma_1 < \gamma_2$, $\gamma_1 = \gamma_2$, or $\gamma_1 > \gamma_2$ is important and we test each. Amplitudes are repeated within the pattern to reduce the possibility that the material would “learn” a 2-cycle trajectory, instead of storing each value indepen-

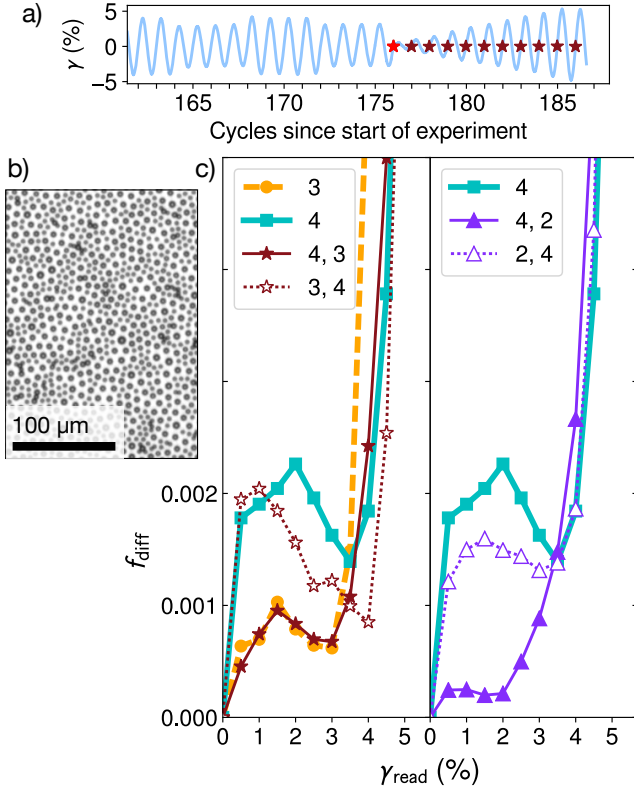


FIG. 1. Training and readout in experiments. **(a)** Shear strain. Training alternates between amplitudes $\gamma_1 = 4\%$ and $\gamma_2 = 3\%$ (small variations are due to the rheometer being primarily stress-controlled). The leftmost star (\star) marks the trained state. During readout, the system’s state at each time marked with a star is compared with the trained state. **(b)** Detail of material. **(c)** *Both panels*: The fraction of particles observed to rearrange in each comparison during readout, as a function of the strain amplitude just applied. Curves are labeled by training protocol, *e.g.* “3” means $\gamma_1 = \gamma_2 = 3\%$; “4, 3” means $\gamma_1 = 4\%$, $\gamma_2 = 3\%$. “4, 3” shows evidence of both memories, but “3, 4” does not.

dently. After ~ 15 cycles the material appears to reach a steady state. At the end of training typically $\lesssim 0.1\%$ of particles rearrange irreversibly per repetition of the 8-cycle pattern, compared with $\sim 20\%$ rearranging and returning to previous positions. γ_2 is always applied last before readout.

The readout protocol in Fig. 1a consists of applying cycles of successively larger amplitude γ_{read} , at values from well below to well above the training values [2, 3, 16]. After each cycle of readout, we compare the system’s state with that at the end of training—the trained state. To find differences we compute each particle’s D_{min}^2 , which identifies particle rearrangements by evaluating whether the motions of the particle and its ~ 20 closest neighbors are non-affine [7, 12, 25]. In our experiments most parts of the material deform elastically, whereas plastic rearrangements are localized in space and time [7, 8, 12]. We

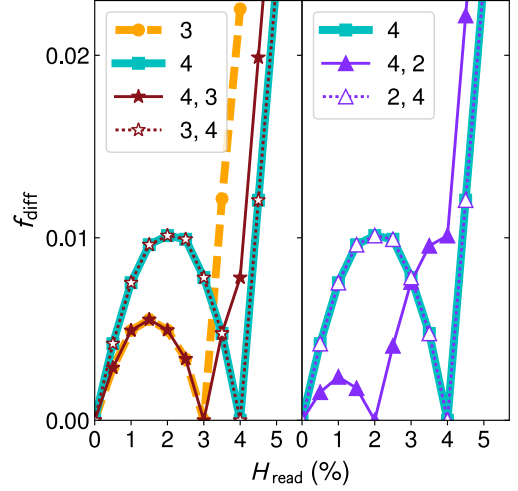


FIG. 2. Readouts of the trained Preisach model. Signals qualitatively match Fig. 1c and more closely match simulations in [15].

say that a particle has rearranged if its $D_{\text{min}}^2 \geq 0.015$, corresponding to a deviation of $\sim 0.1d$ from strictly elastic deformation, where d is the typical spacing between particles. This threshold discriminates well between elastic and plastic regions [12]. Details of these computations are in the Supplemental Materials [22].

When comparing states we measure the fraction of particles with elevated D_{min}^2 , f_{diff} . The readouts in Fig. 1c show f_{diff} as a function of γ_{read} . The “3” and “4” labels refer to single-amplitude training with $\gamma_1 = \gamma_2 = 3\%$ and 4% , respectively. f_{diff} rises as γ_{read} is increased but dips near the training value, after which it rises rapidly. Consistent with other studies [6, 14–16] we also see evidence for multiple memories. The “4, 3” label in Fig. 1c refers to $\gamma_1 = 4\%$, $\gamma_2 = 3\%$; there, we observe a memory at $\gamma_{\text{read}} = 3\%$, but we also see evidence for a memory above 3% , in that f_{diff} more closely follows the “4” curve than the “3” curve. The “4, 2” curve has a similar form. The result is very different when we apply the larger amplitude last (“3, 4” and “2, 4”): the clear signature of the smaller value is gone.

The erasure of smaller memories by larger ones is a feature of return-point memory (RPM). In the present context, RPM means that a cycle with amplitude γ_1 restores the system to the state it had after the previous cycle with γ_1 , so long as strain did not exceed γ_1 in the interim [17, 26]. The restoration erases any memories formed in the interim, in this case the memory of $\gamma_2 = 3\%$ or 2% . In the rest of this paper, we explore the possibility that the behaviors described here and elsewhere are in fact RPM.

We begin with a model known to have RPM, the Preisach model originally used to study hysteresis in ferromagnets [17, 27]. It considers a collection of hysteretic

subsystems, or “hysterons,” each of which is in the “+1” or “-1” state, and is coupled to an external field H . The i th hysteron will “flip” from -1 to +1 when H is increased past H_i^+ ; it will flip back when H is decreased past H_i^- . To show the idealized behavior of the model we use 25,000 hysterons. H_i^+ and H_i^- are distributed uniformly from -0.1 to 0.1 to represent disorder, and hysterons are restricted to the half-plane $H_i^+ > H_i^-$ to represent dissipative dynamics.

Figure 2 shows readouts of the Preisach model, analogous to Fig. 1. Here f_{diff} is the fraction of hysterons that are in a different state than at the end of training—the normalized Hamming distance. While these curves are roughly consistent with our experiments, they are strikingly similar to results from molecular dynamics simulations of amorphous solids [6, 14, 15], where a prominent “kink” signaled the larger memory value, and where the smaller amplitude was always applied last. (In recent bubble raft experiments [16] the larger memory was instead observed as a second minimum, but the annular geometry and use of absolute particle displacements in that work make direct comparisons difficult.)

To better explain the readouts, in Fig. 3 we show the model’s state during training and readout, with hysterons arranged by H_i^+, H_i^- and colored by their states. This illustrates the origins of the “4, 3” curve in Fig. 2. Applying $H_{\text{read}} = 3\%$ restores the trained state, making $f_{\text{diff}} = 0$. The kink as H_{read} passes 4% comes from the many hysterons with $H^+ > 4\%$ or $H^- < -4\%$ that were heretofore inactive. To summarize the kinematics of readout, in Fig. 3f we partition the H^+-H^- plane to show which hysterons are changed by complete cycles with $H_{\text{read}} = 3, 4$, and 5%.

We further test whether RPM is present in experiments by comparing single-particle kinematics with the model, again for the “4, 3” training. We sample whenever $\gamma = 0$, twice per cycle (Fig. 4a), and identify particles that differ from the trained state. Because the D_{min}^2 threshold is a source of noise in these single-particle observations, we ignore particles at the margins of rearranging clusters [22]. Figure 4b shows the states of the ~ 2000 particles that rearrange, and shows that *both* memories are due to RPM: not only does $\gamma_{\text{read}} = 3\%$ restore the corresponding state from training, but $\gamma_{\text{read}} = 4\%$ does as well. As in the Preisach model, we see that the memories are signaled by specific groups of rearrangements. Each group in Fig. 4b is colored according to the region in Fig. 3f that plays the analogous role in the model. It is the entries and exits of these groups that create the signals in Figs. 1c, 2, and 4c. In the inset of Fig. 4b these colors label positions of rearranging particles in a portion of the system. The groupings of colors suggest that persistent clusters of rearranging particles, or distinct regions thereof, are the “hysterons” in this material.

Discussion — By observing the motions of particles we have shown that to a good approximation, the amorphous

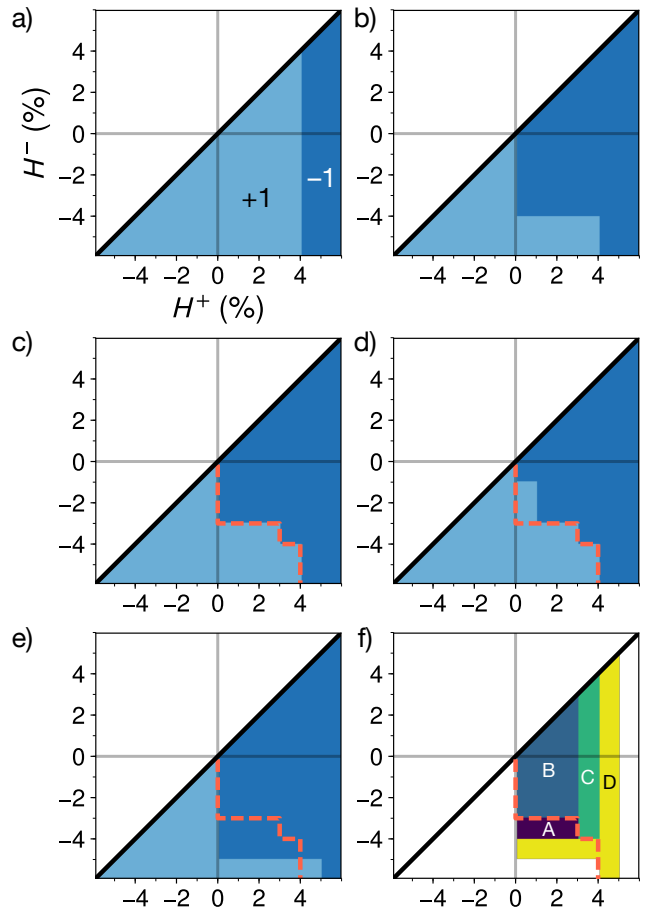


FIG. 3. Training and readout of the Preisach model, corresponding to the “4, 3” curve in Fig. 2. Each panel shows the states of the many hysterons in the system, which have various H^+ and H^- ; colors indicate the +1 and -1 states. (a) System after forward “shear” to $H = 4\%$. Every hysteron with $H^+ \leq 4\%$ is now in the +1 state. (b) Driving to -4% (flipping states according to H^-), then to 0, completes the cycle. (c) A cycle with amplitude 3% adds a memory. Dashed line is the trained boundary that encodes memories. (d) Result of readout cycle with $H_{\text{read}} = 1\%$. f_{diff} is proportional to area between dashed line and actual boundary. Not shown: $H_{\text{read}} = 3\%$, 4% restore states in panels c, b respectively. (e) Once $H_{\text{read}} > 4\%$, f_{diff} grows rapidly on both sides of dashed line. (f) Hysterons labeled according to role in reading out the memory, partitioning the plane according to successive extrema of H : $\pm 3, \pm 4, \pm 5\%$.

solid in our experiment has return-point memory. Our readout protocol, developed elsewhere [2, 3, 16], is in fact a novel method of reading out RPM. This raises the question of how RPM arises from the physics of amorphous solids. In the limit of small strain amplitude γ_0 , the population of rearrangements is dilute. Each cluster of rearranging particles can be approximated as a two-state subsystem that does not interact with its neighbors [7] and switches states at well-defined values of strain [28], realizing the Preisach model. However we believe that at

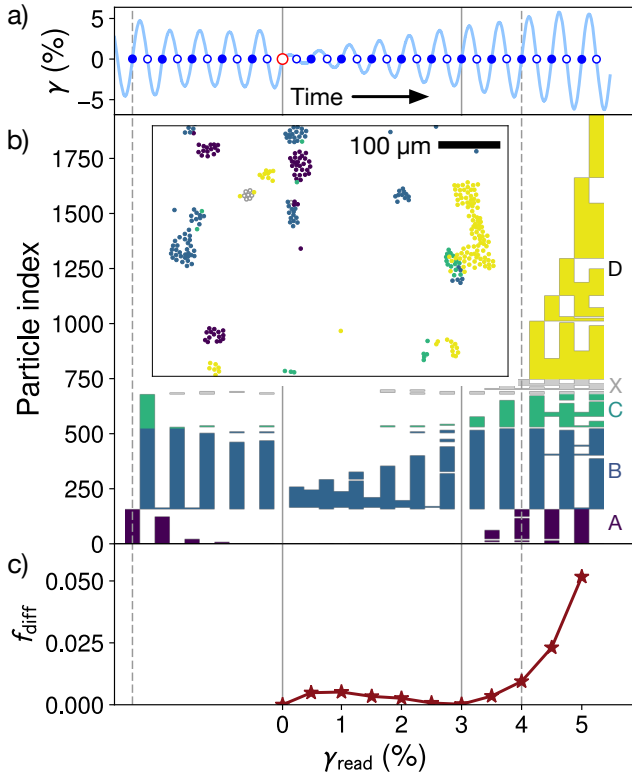


FIG. 4. Training and readout at the level of individual rearrangements of particles, from one of the “4, 3” movies averaged in Fig. 1c. **(a)** Strain for last cycles of training, and readout as in Fig. 1a. Large open red circle indicates trained state; small blue closed and open circles are samples compared to that state. **(b)** For a given particle index (vertical axis) and sample (horizontal axis), a colored bar indicates that particle is in a rearranged state. Particles are ordered, colored, and labeled according to the roles they play in Fig. 3f; only “X” particles cannot be placed. Pairs of solid and dashed vertical lines show how $\gamma_{\text{read}} = 3\%$, 4% restore past states, consistent with RPM. *Inset*: Positions of rearranging particles in a portion of the material. Colors show how memory storage is localized. Gray open circles are “X” particles. **(c)** Readout signal made by counting colored bars in (b).

the γ_0 values we use, rearrangements are not dilute and interactions cannot be ignored [11, 28, 29]: the apparent γ_i^+ , γ_i^- (analogous to H_i^+ , H_i^-) depend on γ_0 , presumably due to other rearrangements becoming active or inactive when γ_0 is varied (Fig. 4b). Because interactions can be “ferromagnetic” (each one encourages others) or “antiferromagnetic,” [29] in general we should not expect exact RPM [26]. Rather than the Preisach model, we can look to studies of disordered magnetic systems more generally, where despite complex interactions RPM may still hold at least approximately [30–32]. Depending on the parameters of driving and disorder, such systems can also exhibit limit cycles with period proliferation (violating RPM) [33], as have been observed in amorphous solids [13, 34]. More relevant to the present experiments,

there is precedent for RPM after a transient [32, 35], which Mungan and Terzi [36] recently developed an abstract way to model using discrete states.

In the magnetic systems just discussed, disorder is quenched—the Hamiltonian prescribes fixed couplings of a constant population of subsystems to each other and an external field—facilitating the system’s return to previous states. But disorder in deformed solids is generally *not* quenched: even in athermal systems, for $\gamma_0 \gtrsim 0.1$ each cycle remodels the material irreversibly [11–13, 37, 38]. Indeed, we use this behavior to randomize the system between experiments. After shearing for many cycles at smaller γ_0 , however, rearrangements become repeatable and new ones are not created [9, 12, 13]. Disorder in our experiments is not quenched but it is nearly *quiescent*. Perfect quiescence is not needed: Fiocco *et al.* [6] found that multiple memories could be read late in the transient, and in the present experiments, external vibrations and slow aging of the interface cause small intermittent changes.

There is one major way our data violate RPM: comparing the “4” curve in Fig. 1b with the “2, 4” and “3, 4” curves suggests that these differently-prepared systems are different, even when RPM states that their memory content must be the same. We surmise that the differences arose during the transient, when disorder was *not* quenched and was shaped by driving. In a separate analysis we have found that for training with two amplitudes, rearrangements are fewer and less hysteretic in the steady state. The trained *population* of rearrangements—not their states—may encode a new, unexplored kind of memory.

The steady state of amorphous solids under cyclic driving has been variously called a “limit cycle,” “periodic,” “cyclic,” “reversibly plastic,” and “loop-reversible” by us and other authors. Each term describes the motions of the particles under periodic shear with constant amplitude, implying that once that amplitude is reduced and the periodicity is broken, the steady state ends. But we have identified an aspect of the system that persists: the hysteretic subsystems that make it possible to recall that same “limit cycle” at a later time. Our results challenge the prevalent conception of these steady states, and may shed light on the physics of marginal stability that underlie them [13].

For illuminating discussions we thank Karin Dahmen, Muhittin Mungan, Sidney Nagel, Srikanth Sastry, Ajay Sood, and Joseph Paulsen. We also thank Paulo Arratia, David Gagnon, Larry Galloway, Luke Horowitz, Dani Medina, and Peter Nelson for their help. Minus K Technology donated the 100BM-1 vibration isolation platform used in experiments. This work was supported by NSF grant DMR-1708870, by an RSCA grant from the California State University, and by NSF grant PHY-1748958 to the KITP.

* nkeim@calpoly.edu

- [1] K. M. Schmoller and A. R. Bausch, *Nat. Mater.* **12**, 278 (2013).
- [2] N. C. Keim and S. R. Nagel, *Phys. Rev. Lett.* **107**, 010603 (2011).
- [3] J. D. Paulsen, N. C. Keim, and S. R. Nagel, *Phys. Rev. Lett.* **113**, 068301 (2014).
- [4] S. N. Coppersmith, T. C. Jones, L. P. Kadanoff, A. Levine, J. P. McCarten, S. R. Nagel, S. C. Venkataramani, and X. Wu, *Phys. Rev. Lett.* **78**, 3983 (1997).
- [5] M. L. Povinelli, S. N. Coppersmith, L. P. Kadanoff, S. R. Nagel, and S. C. Venkataramani, *Phys. Rev. E* **59**, 4970 (1999).
- [6] D. Fiocco, G. Foffi, and S. Sastry, *Phys. Rev. Lett.* **112**, 025702 (2014).
- [7] M. L. Falk and J. S. Langer, *Annu. Rev. Condens. Matter Phys.* **2**, 353 (2011).
- [8] E. D. Cubuk, R. J. S. Ivancic, S. S. Schoenholz, D. J. Strickland, A. Basu, Z. S. Davidson, J. Fontaine, J. L. Hor, Y. R. Huang, Y. Jiang, N. C. Keim, K. D. Koshygan, J. A. Lefever, T. Liu, X. G. Ma, D. J. Magagnosc, E. Morrow, C. P. Ortiz, J. M. Rieser, A. Shavit, T. Still, Y. Xu, Y. Zhang, K. N. Nordstrom, P. E. Arratia, R. W. Carpick, D. J. Durian, Z. Fakhraai, D. J. Jerolmack, D. Lee, J. Li, R. Riggelman, K. T. Turner, A. G. Yodh, D. S. Gianola, and A. J. Liu, *Science* **358**, 1033 (2017).
- [9] I. Regev, T. Lookman, and C. Reichhardt, *Phys. Rev. E* **88**, 062401 (2013).
- [10] N. C. Keim and P. E. Arratia, *Soft Matter* **9**, 6222 (2013).
- [11] K. H. Nagamanasa, S. Gokhale, A. K. Sood, and R. Ganapathy, *Phys. Rev. E* **89**, 062308 (2014).
- [12] N. C. Keim and P. E. Arratia, *Phys. Rev. Lett.* **112**, 028302 (2014).
- [13] I. Regev, J. Weber, C. Reichhardt, K. A. Dahmen, and T. Lookman, *Nat. Comms.* **6**, 8805 (2015).
- [14] D. Fiocco, G. Foffi, and S. Sastry, *J. Phys: Cond. Matter* **27**, 194130 (2015).
- [15] M. Adhikari and S. Sastry, *Eur. Phys. J. E* **41**, 045504 (2018).
- [16] S. Mukherji, N. Kandula, A. K. Sood, and R. Ganapathy, *arXiv:1808.07701* (2018).
- [17] J. Barker, D. Schreiber, B. Huth, and D. H. Everett, *Proc. R. Soc. Lond. A* **386**, 251 (1983).
- [18] K. Masschaele, B. J. Park, E. M. Furst, J. Fransaer, and J. Vermant, *Phys. Rev. Lett.* **105**, 048303 (2010).
- [19] I. Buttinoni, Z. A. Zell, T. M. Squires, and L. Isa, *Soft Matter* **11**, 8313 (2015).
- [20] C. F. Brooks, G. G. Fuller, C. W. Frank, and C. R. Robertson, *Langmuir* **15**, 2450 (1999).
- [21] S. Reynaert, C. F. Brooks, P. Moldenaers, J. Vermant, and G. G. Fuller, *J. Rheol.* **52**, 261 (2008).
- [22] See Supplemental Material for additional details of methods.
- [23] J. C. Crocker and D. G. Grier, *J. Colloid Interf. Sci.* **179**, 298 (1996).
- [24] D. B. Allan, T. Caswell, N. C. Keim, and C. M. van der Wel, “Trackpy v0.4.1,” DOI:10.5281/zenodo.1226458 (2018).
- [25] N. C. Keim, “Philatracks v0.2,” DOI:10.5281/zenodo.11459 (2014).
- [26] J. P. Sethna, K. Dahmen, S. Kartha, J. A. Krumhansl, B. W. Roberts, and J. D. Shore, *Phys. Rev. Lett.* **70**, 3347 (1993).
- [27] F. Preisach, *Z. Physik* **94**, 277 (1935).
- [28] N. Perchikov and E. Bouchbinder, *Phys. Rev. E* **89**, 062307 (2014).
- [29] G. Picard, A. Ajdari, F. Lequeux, and L. Bocquet, *Eur. Phys. J. E* **15**, 371 (2004).
- [30] J. M. Deutsch, A. Dhar, and O. Narayan, *Phys. Rev. Lett.* **92**, 227203 (2004).
- [31] M. S. Pierce, C. R. Buechler, L. B. Sorensen, J. J. Turner, S. D. Kevan, E. A. Jagla, J. M. Deutsch, T. Mai, O. Narayan, J. E. Davies, K. Liu, J. H. Dunn, K. M. Chesnel, J. B. Kortright, O. Hellwig, and E. E. Fullerton, *Phys. Rev. Lett.* **94**, 017202 (2005).
- [32] O. Hovorka and G. Friedman, *Phys. Rev. Lett.* **100**, 097201 (2008).
- [33] J. M. Deutsch and O. Narayan, *Phys. Rev. Lett.* **91**, 3 (2003).
- [34] M. O. Lavrentovich, A. J. Liu, and S. R. Nagel, *Phys. Rev. E* **96**, 020101 (2017).
- [35] I. Gilbert, G.-W. Chern, B. Fore, Y. Lao, S. Zhang, C. Nisoli, and P. Schiffer, *Phys. Rev. B* **92**, 104417 (2015).
- [36] M. Mungan and M. M. Terzi, *arXiv:1802.03096* (2018).
- [37] P. Hébraud, F. Lequeux, J.-P. Munch, and D. J. Pine, *Phys. Rev. Lett.* **78**, 4657 (1997).
- [38] N. V. Priezjev, *Phys. Rev. E* **87**, 052302 (2013).